Journal of Thermal Analysis, Vol. 42 (1994) 343-359

THERMAL BEHAVIOUR OF SULPHATO AND NITRATO COMPLEXES OF CERIUM(IV)

G. Pokol T. Leskelä and L. Niinistö*

Laboratory of Inorganic and Analytical Chemistry, Helsinki University of Technology,
FIN - 02150 Espoo, Finland

Abstract

Four sulphato and nitrato complexes of cerium(IV), *viz.* $(NH_4)_4Ce(SO_4)_4 \cdot 2H_2O$ (**1**), $(NH_4)_2Ce(SO_4)_3$ (**2**), $(NH_4)_2Ce(NO_3)_6$ (**3**) and $Cs_2Ce(NO_3)_6$ (**4**) were studied by simultaneous TG/DTA under various experimental conditions in order to establish their decomposition mechanism and to compare the results with the literature data which have been reviewed. In the case of the ammonium compounds (**1**, **2** and **3**) the decompositions are accompanied by changes in the oxidation state of cerium; the presence of Ce(III) and Ce(IV) were studied by *ex situ* magnetic susceptibility and XPS measurements. The crystal structure of (**1**) was determined as well. It forms monoclinic crystals with space group $P2_1/c$; the parameters of the unit cell are: a = 12.638(18) Å, b = 11.362(10) Å, c = 13.607(11) Å, β = 110.17(9)°, V = 1834.05 Å^3.

Keywords: Ce(IV) compounds, magnetic susceptibility, thermal analysis, XPS

Introduction

Existing and expected applications of rare earth compounds as superconductors, components or additives in catalysts, in thin films for electronic and optoelectronic devices, etc. have resulted in an increasing interest in the properties and reactions of rare earth complexes because of their potential use as precursors for those materials. Earlier in our laboratory some rare earth sulfato and nitrato complexes have been structurally and thermally characterized, *e.g.*

---

* Permanent address: Institute for General and Analytical Chemistry, Technical University of Budapest, H-1521 Budapest, Hungary

0368–4466/94/ $ 4.00

John Wiley & Sons, Limited, Chichester
Akadémiai Kiadó, Budapest

$NH_4Sm(SO_4)_2{\cdot}4H_2O$ [1] and $(NH_4)_2La(NO_3)_5{\cdot}nH_2O$ (n = 3, 4) [2], and the structural, physical and chemical properties of inorganic complexes of rare earths have been reviewed in detail [3, 4].

In the present paper we report on the thermal decomposition and structural characteristics of four inorganic complexes of cerium(IV) where ammonium and cesium act as counter ions, *viz.* $(NH_4)_4Ce(SO_4)_4{\cdot}2H_2O$ (**1**), $(NH_4)_2Ce(SO_4)_3$ (**2**), $(NH_4)_2Ce(NO_3)_6$ (**3**) and $Cs_2Ce(NO_3)_6$ (**4**). Because of the partly contradictory reports, the literature is reviewed in sufficient detail in order to facilitate a comparison of the present results with the earlier investigations.

Literature survey

Ammonium sulphates of Ce(IV)

Tetraammonium cerium(IV) sulphate dihydrate (**1**), being a well-defined and stable compound may be used as a starting material for syntheses requiring cerium(IV). It is also being used as an oxidizing agent. Its crystal structure has not been described in the literature. The potassium analog belongs to the $P2_1/c$ space group and contains nine-coordinated cerium(IV) ions [5].

Several other ammonium cerium(IV) sulphates exist [6]: (**2**) and its tri- and dihydrate, $(NH_4)_6Ce(SO_4)_5{\cdot}3H_2O$, $(NH_4)_8Ce(SO_4)_6{\cdot}nH_2O$ (n = 3, 5) and $(NH_4)_{10}Ce(SO_4)_7{\cdot}3H_2O$. The crystal structures of these compounds have not been described either. The cesium analog of $(NH_4)_2Ce(SO_4)_3$, *i.e.*, $Cs_2Ce(SO_4)_3$, crystallizes in the space group $P2_1$; half of the cerium ions are octacoordinated while the other half is nine-coordinated [7].

Since the early 60s, several reports have been published on the thermal behaviour of (**1**), where the loss of the two water molecules is the first step [8, 9]. The further degradation (which is clearly separated from the dehydration) consists of several steps, and the final product at about 900°C is cerium(IV) oxide [6]. However, there are contradicting results and conclusions on the decomposition steps and intermediates. In the early studies it was concluded that the plateau in the TG curve at 550–700°C corresponded to an intermediate with the composition $3CeO_2{\cdot}4SO_3$ (expressed also as $2Ce(SO_4)_2{\cdot}CeO_2$ or $Ce_3O_2(SO_4)_4$ [6, 8–10]. The occurrence of cerium(IV) sulphate was regarded probable during the formation of this intermediate [10].

Quite detailed investigations on (**1**) were carried out by Bondar *et al.* [11]. On the basis of TG and DTA curves as well as IR spectra and chemical analysis of the intermediate products, the following reaction path was put forward (note the decrease and subsequent increase of cerium oxidation state):

$$2(NH_4)_4Ce(SO_4)_4{\cdot}2H_2O \rightarrow 2(NH_4)_4Ce(SO_4)_4 \rightarrow$$

$$(NH_4)_2S_2O_7 + 2NH_4HSO_4 + 2NH_4Ce(SO_4)_2 \rightarrow$$

$$2NH_4Ce(SO_4)_2 \rightarrow Ce_2(SO_4)_3 \rightarrow 2CeO_2 \qquad (1)$$

IR spectra were used to identify $NH_4Ce(SO_4)_2$ and the disulphate ion. The article, however, fails to establish which species is oxidized during the reduction of Ce(IV); the evolution of ammonia and water is only mentioned in the second transformation.

Ce(IV) → Ce(III) → Ce(IV) transition had been included earlier in the thermal decomposition schemes of various cesium cerium sulphates as well [12]. Here the evolution of elementary oxygen was detected by mass spectrometry during the cerium reduction.

House and Kemper [13] also assumed the formation of disulphate. The reaction sequence proposed by them was based on the mass loss ratios:

$$(NH_4)_4Ce(SO_4)_4{\cdot}2H_2O \rightarrow (NH_4)_4Ce(SO_4)_4 \rightarrow$$

$$CeSO_4S_2O_7 \rightarrow Ce(SO_4)_2 \qquad (2)$$

More recently, TG, DTA as well as elemental analysis and magnetic susceptibility measurements of 5 products formed during heating of **1** were applied by Sharma *et al.* [14]. In agreement with Bondar *et al.* [11, 12] they concluded that Ce(III) was formed during the decomposition but that the final product contained tetravalent cerium. Two intermediate phases $(NH_4)_3Ce(SO_4)_{3.5}$ and $NH_4Ce(SO_4)_2$ were proposed [14]. In a recent work dealing with the thermal decomposition of $Ce(SO_4)_2{\cdot}4H_2O$ [15], anhydrous cerium(IV) sulphate and, subsequently, cerium(III) sulphate were found as intermediates; cerium(IV) oxide was the final product. The changes in the oxidation state were confirmed by magnetic moment measurements.

It is worth mentioning here that changes in the oxidation state of cerium(IV) have been reported in other systems, too. Examples include the reaction of CeO_2 with ammonium dihydrogen phosphate [16] and Pd–Ce catalysts [17]. Other XPS [18–20] and X-ray absorption studies [21, 22] also revealed a mixed oxidation state in formally tetravalent cerium compounds and their thermal decomposition products. Cerium in the final product CeO_2 was generally found or regarded clearly tetravalent. However, a mixed oxidation state was suggested in Refs [20, 22].

On the other hand (2) itself has not been studied by thermoanalytical techniques, but it was found to occur as an intermediate in the decomposition of corresponding hydrates. Thus, $(NH_4)_2Ce(SO_4)_3{\cdot}3H_2O$ transforms first to the dihydrate upon heating, then loses the remaining two water molecules yielding (2) [9]. According to a recent report, the anhydrous phase also occurred as a stable intermediate when the cerium(III) complex $NH_4Ce(SO_4)_2{\cdot}H_2O$ was heated [23].

Ammonium nitrates of Ce(IV)

Among complexes of tetravalent cerium, ammonium cerium nitrate (**3**) is of special importance. It has been used as an oxidizing agent in reactions of organic compounds, as an initiator in polymerization and graft copolymerization processes and as a precursor for cerium-containing catalysts. Besides, standard solutions of cerium(IV) for cerimetry are made of (**3**). It forms crystals in the space group $P2_1/n$; the structure contains 12-coordinated Ce atoms with six bidentate nitrato groups [24].

The first detailed study on the thermal decomposition of ammonium cerium nitrate was reported by Brezina and Rosicky [25]. According to their observations, (3) decomposed at 185–340°C, corresponding to Eq. (3):

$$(NH_4)_2Ce(NO_3)_6 \rightarrow 2N_2O + 4H_2O + CeO_2 + 4NO_2 + O_2 \qquad (3)$$

In the decomposition of the potassium and cesium analogs, alkali nitrates and Ce(IV) oxide were the products:

$$M_2Ce(NO_3)_6 \rightarrow 2MNO_3 + CeO_2 + 4NO_2 + O_2\ (M = \mathrm{K, Cs}) \qquad (4)$$

The decomposition of potassium nitrate and cesium nitrate was reported to commence at 450 and 510°C, respectively. Though the TG curves indicated several overlapping steps, the authors concluded that the thermal decomposition of the starting complexes directly yielded CeO_2. However, $(NH_4)HCe(NO_3)_6$ and $CeO(NO_3)_2$ were proposed by Zaki and Baird [26] as intermediates of (**3**) decomposition.

The occurrence of intermediates has been debated in the case of simple cerium nitrates, as well. In his pioneering study, Wendlandt [27] found no mass plateaus in the thermal decomposition of cerium(III) nitrate hexahydrate; after a gradual loss of water and nitrogen oxides he obtained CeO_2 at 450°C. Thermal reactions of cerium(III) nitrate hydrates were also investigated by Pajakoff [28] in oxygen. On the basis of chemical analysis cerium(IV) compounds: $Ce(NO_3)_4$ and $CeO(NO)_3)_2$ were proposed as intermediates. Claudel *et al.* [29] as well as Molodkin *et al.* [30] did not find any oxonitrate intermediate in the thermolysis of cerium(III) nitrate hexahydrate. A similar conclusion was later drawn by Strydom and van Vuuren [31] as well as by Ivanov-Emin and Medvedev [32] who started from the anhydrous compound. It is relevant to mention, however, that other Ln(III) nitrates have been reported to decompose *via* oxonitrate intermediates [27, 31, 33].

In view of the complex reaction mechanisms and contradicting literature data, it was decided to undertake the present study involving four Ce(IV) complexes. The compounds were first structurally characterized when no data existed. The intermediate phases and final products were identified by *ex situ* experiments involving magnetic susceptibility measurements, XPS and XRD. The cesium complex (**4**), expected to be isostructural with (**3**) was used for comparative studies in order to find out the possible reducing effect of ammonium ions in the decomposition.

Experimental

Analytical grade ammonium cerium(IV) sulphate dihydrate, $(NH_4)_4Ce(SO_4)_4 \cdot 2H_2O$, (Merck, Art. No. 2273) was used as the starting material to prepare (**1**). For structural investigations it was dissolved in 3% sulphuric acid solution and recrystallized at 80°C after partial evaporation of water. Of this batch, some single crystals were selected for the structure determination while the remaining part was used after grinding for thermoanalytical and X-ray powder diffraction measurements. (**2**) was prepared from (**1**) which was dissolved in 20% sulphuric acid and recrystallized at 100°C. It was also investigated by thermoanalytical and X-ray diffraction methods.

Ammonium cerium(IV) nitrate (**3**) was recrystallized from an analytical grade commercial reagent (Merck, Art No. 2276). Cesium cerium(IV) nitrate (**4**) was obtained from $Ce(OH)_4$ and $CsNO_3$ by the procedure described in Ref. [25].

Single crystal X-ray diffraction data were measured on a Syntex *P*2$_1$ diffractometer, and the calculations were carried out with the aid of program package SHELX-76. In the X-ray analysis of powder samples, a Philips MPD 1880 diffractometer with CuK_α radiation was used.

Simultaneous TG and DTA curves were recorded in a Seiko 320 instrument belonging to the SSC 5200 series both in flowing air and nitrogen atmospheres. Sample mass was 5–7 mg; 10 and 2 deg·min^{-1} heating rates were applied. For the analysis of the evolved gases, a TG–MS system assembled in our laboratory [34] and a commercial TG–IR apparatus were applied. The sample size in the former system was 60–70 mg and the heating rate was 10 deg·min^{-1}. The coupled TG–FTIR runs were carried out in a BOMEM TG/Plus system consisting of a DuPont 951 thermobalance and a BOMEM MB 102 FTIR spectrometer. In these experiments, 120 mg samples were heated at 10 deg·min^{-1} in flowing helium and spectra were recorded every 30 s.

For *ex situ* studies on intermediate and final products, the starting material was treated isothermally at temperatures determined on the basis of the TG runs. The samples obtained in this way were characterised by magnetic susceptibility measurements, XPS and XRD. In the determination of magnetic moments an Oxford Instruments Faraday balance was applied. 10 mg samples were measured at room temperature in fields of 0.5 and 0.8 *T*. XPS spectra were recorded with a VG ESCA 200 instrument using monochromatized AlK$_\alpha$ radiation.

Results and discussion

Structure and thermal decomposition of ammonium cerium(IV) sulphates

According to the results of X-ray diffraction analysis, the single crystals of $(NH_4)_4Ce(SO_4)_4 \cdot 2H_2O$ were monoclinic, space group $P2_1/c$. The parameters of the unit cell and their corresponding standard deviations (in parentheses) are as follows: a = 12.638(18) Å, b = 11.362(10) Å, c = 13.607(11) Å, β = 110.17(9)° and V = 1834.05 Å^3. These values are very close to the unit cell parameters of $K_4Ce(SO_4)_4 \cdot 2H_2O$ (a = 12.407 Å b = 11.160 Å, c = 13.579 Å, β = 111.63°, V = 1747.78 Å^3 [5], *i.e.*, the two solids appear isostructural. A detailed description of the crystal structure of (1) will be presented elsewhere [35].

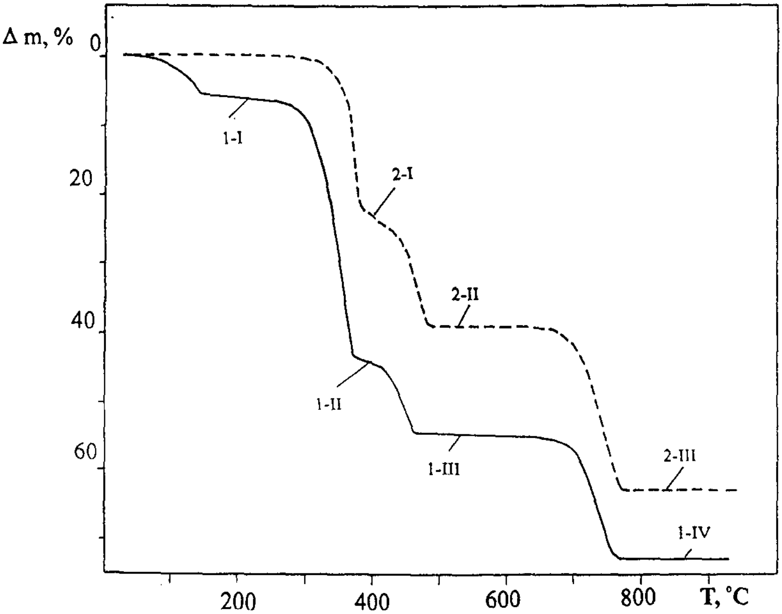

Fig. 1 TG curves of $(NH_4)_4Ce(SO_4)_4 \cdot 2H_2O$ (1) and $(NH_4)_2Ce(SO_4)_3$ (2) recorded in flowing nitrogen with 10 deg·min^{-1} heating rate. For the suggested compositions at the indicated points, Tables 1 and 2

Figure 1 shows the TG curves of the two ammonium cerium(IV) sulphates. On the TG curves, roman numerals (following the code of the substance used in the text) are assigned to the plateaus and inflexions. Tables 1 and 2 contain the mass percentages belonging to the points selected on the basis of the DTG curves, as well as compositions of the proposed intermediates and products. In all tables the temperatures are rounded to nearest five degrees. Theoretical mass ratios are also included. The shape of the TG curves and the weight loss data were practically independent of the atmosphere used (inert or oxidative).

Table 1 Evaluation of the TG curves of $(NH_4)_4Ce(SO_4)_4 \cdot 2H_2O$ (Fig. 1)

Point no.	Temperature °C	Mass remaining / %	Proposed composition	Theoretical residue / %
1–I	165	93.8	$(NH_4)_4Ce(SO_4)_4$	94.3
1–II	385	55.9	$(NH_4)Ce(SO_4)_2$	55.3
1–III	485	45.1	$Ce(SO_4)_{3/2}$	44.9
1–IV	>800	27.3	CeO_2	27.2

Table 2 Evaluation of the TG curves of $(NH_4)_2Ce(SO_4)_3$ (Fig. 1)

Point no.	Temperature °C	Mass remaining / %	Proposed composition	Theoretical residue / %
2–I	395	76.3	$(NH_4)Ce(SO_4)_2$	75.4
2–II	505	60.6	$Ce(SO_4)_{3/2}$	61.2
2–III	>800	36.7	CeO_2	37.1

In the case of (1), the first process is dehydration (Figs 1 and 2). $NH_4Ce(SO_4)_2$ and $Ce_2(SO_4)_3$ are then formed and indicated by the second and the third plateau of the TG curve. The presence of paramagnetic cerium(III) was confirmed by the magnetic moment values as can be seen in Table 3. The final product (1–IV) is cerium(IV) oxide, which was confirmed by XRD.

Accordingly, the following scheme may be proposed for the decomposition reaction sequence for (1):

$$(NH_4)_4Ce(SO_4)_4 \cdot 2H_2O \rightarrow (NH_4)_4Ce(SO_4)_4 + 2H_2O \quad 40\text{–}160^\circ C \qquad (5)$$

$$(NH_4)_4Ce(SO_4)_4 \rightarrow (NH_4Ce(SO_4)_2 + H_2O, NH_3, NO_x, SO_3, O_2 \quad 240\text{–}380^\circ C \qquad (6)$$

$$NH_4Ce(SO_4)_2 \rightarrow Ce(SO_4)_{3/2} + 1/2H_2O + NH_3 + 1/2SO_3 \quad 410\text{–}470^\circ C \qquad (7)$$

$$Ce(SO_4)_{3/2} \rightarrow CeO_2 + 1/2SO_2 + SO_3 \quad 630\text{–}770^\circ C \qquad (8)$$

The temperature ranges in Eqs (5–8) correspond to the TG curves recorded at the 10 deg·min^{-1} heating rate. Note that the scheme assumes a

Ce(IV) → Ce(III) → Ce(IV) reduction/oxidation sequence, similar to the models presented in Refs [11, 12, 14]. In Eq. (6), only a list of possible products is given without a quantitative evaluation. Ammonia, most likely, plays a role in cerium reduction. Furthermore, the ratio of the gaseous products in a dynamic system is not relevant for composition of the condensed phase. $(NH_4)_2SO_4$, however, may be present during the reaction as its decomposition takes place in that temperature range [36].

Table 3 Magnetic moments of ammonium cerium(IV) sulphate and decomposition products. $(NH_4)_4Ce(SO_4)_4{\cdot}2H_2O$ may be used as reference substance for cerium(IV); for cerium(III) $Ce(NO_3)_3{\cdot}6H_2O$ was measured as standard and a magnetic moment of 2.2 B.M. was obtained

Composition	Corresponding point in Fig. 1	Magnetic moment / B.M.	Qualitative description
$(NH_4)_4Ce(SO_4)_4{\cdot}2H_2O$	–	0.0	diamagnetic
$(NH_4)_4Ce(SO_4)_4$	1–I	0.0	diamagnetic
$(NH_4)Ce(SO_4)_2$	1–II, 2–I	1.95	paramagnetic
$Ce(SO_4)_{3/2}$	1–III, 2–II	2.08	paramagnetic

The decomposition of (2) proceeded in a similar way, *i.e.* compositions $NH_4Ce(SO_4)_2$, $Ce_2(SO_4)_3$ and CeO_2 may be assigned to stages 2-I, 2-II and 2-III, respectively. The first decomposition step at 300–395°C may be written as follows

$$(NH_4)_2Ce(SO_4)_3 \rightarrow NH_4Ce(SO_4)_2 + 1/2H_2O + NH_3 + SO_3 + 1/4O_2 \qquad (9)$$

The next steps are identical with Eqs (7) and (8) though process (7) became complete at a temperature slightly higher (490°C) than in the case of $(NH_4)_4Ce(SO_4)_4{\cdot}2H_2O$.

The results of TG–IR runs are in agreement with the reaction schemes described above. The evolution of the gas phase products of reactions (5–9) were detected in the relevant temperature ranges. Reaction (5) was accompanied by water evolution. In the temperature ranges belonging to reactions (6), (7) and (9), water, ammonia and sulphur oxide peaks were observed. Sulphur oxides were the only detected products of process (8). One should note, however that the IR gas analysis cannot detect oxygen or separate the various sulphur oxides.

Relatively weak signals were obtained for the decomposition products in the TG–MS assembly [34] and the peaks became very broad in comparison to TG. This made the assignment of the signal to a particular step of the decomposition quite difficult. It is worth mentioning, however, that oxygen evolution was detected in the temperature range corresponding to steps (6) and (7). The weak

MS signals are most likely caused by ammonium sulphate condensation in the heated connecting capillary. For comparison, cerium(IV) sulphate tetrahydrate was measured under the same conditions, and satisfactory peaks were detected at the proper decomposition steps for m/e = 32, 48, and 64 corresponding to O_2, SO and SO_2, respectively.

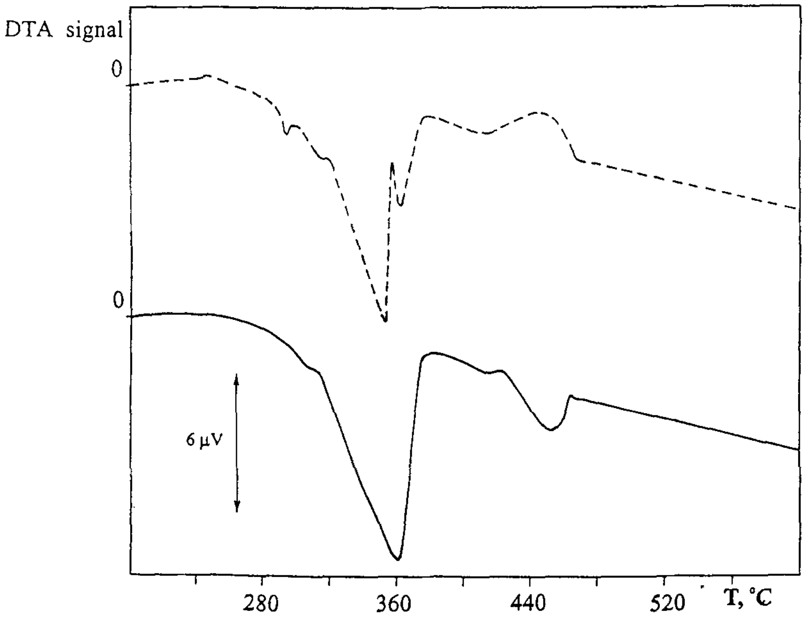

Fig. 2 DTA peaks of $(NH_4)_4Ce(SO_4)_4{\cdot}2H_2O$ (**1**) related to the loss of ammonia in air (- - - -) and nitrogen (———); heating rate: 10 deg·min^{-1}

The simultaneous TG–DTA measurements on (**1**) and (**2**) were run in flowing air as well. The overall shape of the TG curves did not depend on the atmosphere, the residual mass values being virtually identical with those summarized in Tables 1 and 2. However, DTA curves indicated differences in the endothermic/exothermic character of the decomposition steps leading to $NH_4Ce(SO_4)_2$ and $Ce(SO_4)_{3/2}$. The DTA curves of (**1**) are presented in Fig. 2. The intensity and the area of the endothermic peak around 360°C was smaller in air than in nitrogen and in air it was split. Moreover, the next process became exothermic when carried out in air. Taking into account that practically no difference was observed regarding the condensed phase, the changes in the heat effect may be attributed to the oxidation of evolved ammonia. This reaction is catalysed by the platinum sample holder [10].

Thermal decomposition of ammonium and cesium nitrates of cerium(IV)

Figure 3 shows TG curves of (**3**) run in flowing nitrogen with two heating rates. The weak inflexions of the TG curve can only roughly be assigned to stoichiometric intermediates and their isolation is impossible. Moreover, the volatilization of ammonium nitrate formed in the decomposition may also influence the shape of the curves.

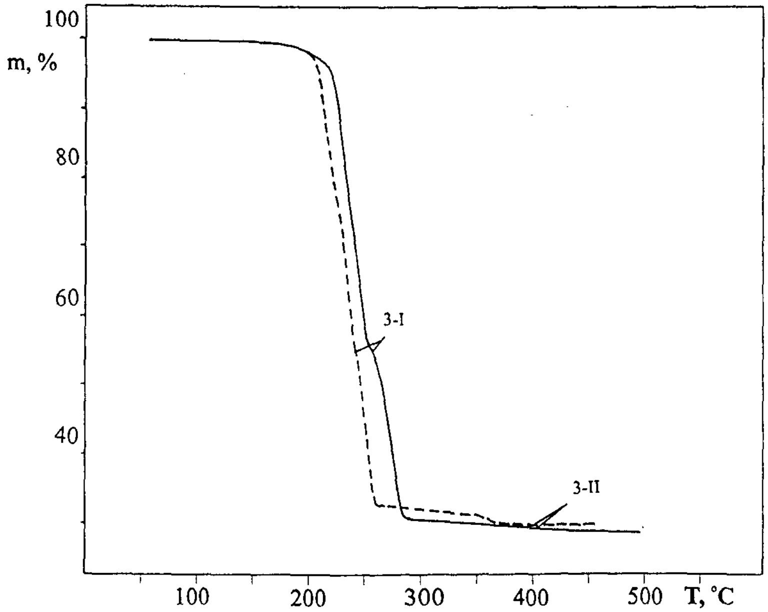

Fig. 3 TG curves of $(NH_4)_2Ce(NO_3)_6$ (**3**) in flowing nitrogen with 10 deg·min^{-1} (——) and 2 deg·min^{-1} (- - - -) heating rate. For the suggested composition at the indicated points, Tables 4 and 5

The *ex situ* measurements were used to resolve the oxidation states of the intermediates. Thus, (**3**) was isothermally processed at 210°C for 2 h in order to prepare a sample corresponding to intermediate **3**-I (Fig. 3 and Tables 4 and 5). The obtained susceptibility confirmed the presence of paramagnetic cerium(III). Consequently, the following reaction sequence is proposed for the thermal decomposition of (**3**):

$$(NH_4)_2Ce(NO_3)_6 \rightarrow Ce(NO_3)_3 \quad 170\text{–}255^{\circ}C \qquad (10)$$

$$Ce(NO_3)_3 \rightarrow CeO_2 \text{ and/or } CeO_{1.5} \quad 255\text{–}290^{\circ}C \qquad (11)$$

When the cesium compound (**4**) was studied by TG/DTA (Figs 4, 5 and Tables 6, 7) there were some temperature differences in runs carried out in nitro-

Table 4 Evaluation of the TG curves of $(NH_4)_2Ce(NO_3)_6$ recorded with a heating rate of 10 deg·min^{-1} (Fig. 3). a – in nitrogen; b – in air. In Fig. 3 only the a-curve is depicted

Point no.	Temperature / °C	Mass remaining / %	Proposed composition	Theoretical residue / %
3–I a	255	55.6	$Ce(NO_3)_3$	59.5
3–I b	255	57.0		
3–II a	480	28.9	CeO_2	31.4
3–II b	480	29.3		

Table 5 Evaluation of the TG curves of $(NH_4)_2Ce(NO_3)_6$ recorded with a heating rate of 2 deg·min^{-1} (Fig. 3). a – in nitrogen; b – in air. In Fig. 3 only the a-curve is shown

Point no.	Temperature / °C	Mass remaining / %	Proposed composition	Theoretical residue / %
3–I a	240	55.1	$Ce(NO_3)_3$	59.5
3–I b	240	53.3		
3–II a	400	30.0	CeO_2	31.4
3–II b	570	29.9		

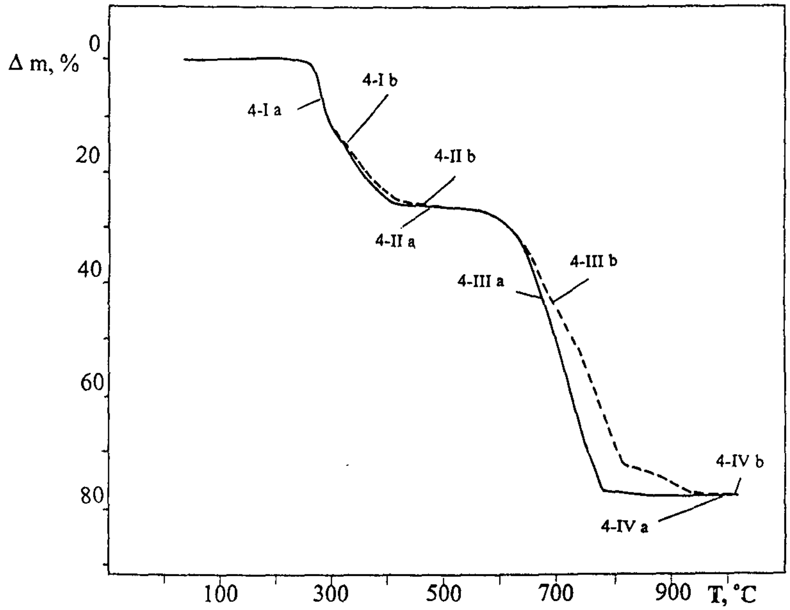

Fig. 4 TG curves of $Cs_2Ce(NO_3)_6$ (4) recorded with a heating rate of 10 deg·min^{-1} in nitrogen (——) and air (- - - -). For the suggested compositions at the indicated points, Table 6

gen but the TG data in air were remarkably similar. TG curves recorded with 10 deg·min^{-1} and 2 deg·min^{-1} heating rates are presented in Figs 4 and 5, respectively. The decomposition reactions covered a wide temperature range. With both heating rates, the process above 600°C was affected by changing the atmosphere from inert gas to air. Further studies are required in order to identify the intermediate appearing in the TG curves recorded in air just before the final product. The parameters of characteristic points of the curves are summarized in Tables 6 and 7. Based on stoichiometry, a cesium cerium(IV) oxonitrate may be proposed as the first intermediate.

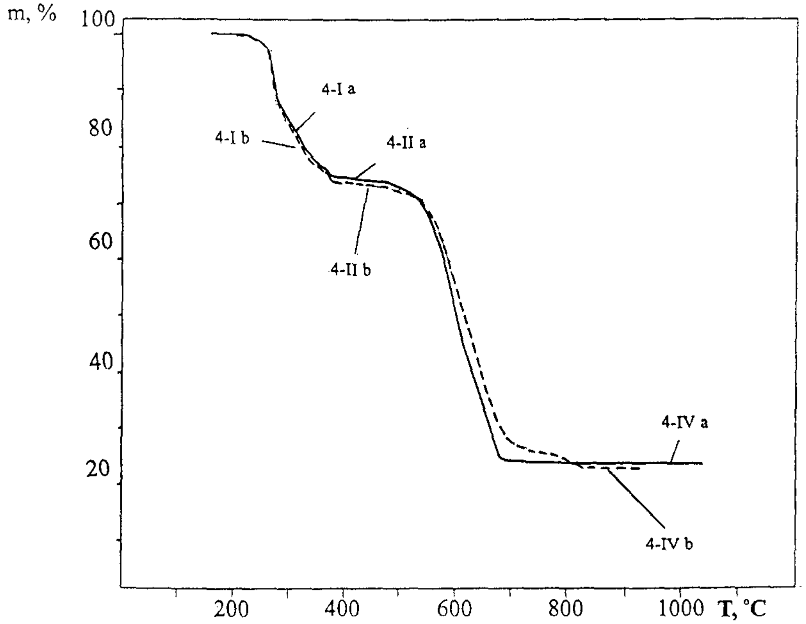

Fig. 5 TG curves of $Cs_2Ce(NO_3)_6$ (4) recorded with a heating rate of 2 deg·min^{-1} in nitrogen (———) and air (- - - -). For the suggested compositions at the indicated points, Table 7

In order to determine whether cerium(III) occurs in the intermediates of cesium cerium(IV) nitrate thermal decomposition, (4) was thermally treated in air at 360°C for 8 h and at 450°C for 2 h. The products corresponded to a mixture of intermediates **4**-I and **4**-II in the first case and to stage **4**-II in the second case. Both products were found to be diamagnetic. Accordingly, cerium is in the +4 oxidation state throughout the thermal decomposition of (**4**) and the following reaction products may be suggested:

$$Cs_2Ce(NO_3)_6 \rightarrow Cs_2CeO(NO_3)_4 \quad 220\text{–}285°C \qquad (12)$$

$$Cs_2CeO(NO_3)_4 \rightarrow Cs_2CeO_2(NO_3)_2 \quad 285–440°C \tag{13}$$

$$Cs_2CeO_2(NO_3)_2 \rightarrow Cs_2CeO_3 \quad 500–690°C \tag{14}$$

$$Cs_2CeO_3 \rightarrow CeO_2 \quad 690–1000°C \tag{15}$$

The approximate temperature ranges indicated in Eqs (10–15) belong to the 10 deg·min^{-1} heating rate.

Table 6 Evaluation of the TG curves of $Cs_2Ce(NO_3)_6$ recorded with a heating rate of 10 deg·min^{-1} (Fig. 4). a – in nitrogen; b – in air

Point no.	Temperature / °C	Mass remaining / %	Proposed composition	Theoretical residue / %
4–I a	285	89.7	$Cs_2CeO(NO_3)_4$	86.1
4–I b	285	90.1		
4–II a	455	73.6	$Cs_2CeO_2(NO_3)_2$	72.2
4–II b	475	73.5		
4–III a	675	54.3	Cs_2CeO_3	58.3
4–III b	685	55.5		
4–IV a	1000	21.2	CeO_2	22.1
4–IV b	1000	21.0		

Table 7 Evaluation of the TG curves of $Cs_2Ce(NO_3)_6$ recorded with a heating rate of 2 deg·min^{-1} (Fig. 5). a – in nitrogen; b – in air

Point no.	Temperature / °C	Mass remaining / %	Proposed composition	Theoretical residue / %
4–I a	290	86.2	$Cs_2CeO(NO_3)_4$	86.1
4–I b	290	84.8		
4–II a	430	74.3	$Cs_2CeO_2(NO_3)_2$	72.2
4–II b	440	73.1		
4–IV a	1000	22.5	CeO_2	22.1
4–IV b	940	21.6		

The difference between the decomposition of ammonium cerium(IV) nitrate and cesium cerium(IV) nitrate with regard to the oxidation state of cerium can be attributed to the presence of ammonium as a counter ion in (**3**), acting as a reducing agent. When comparing the thermal behaviour of the nitrato complexes with that of the sulphate compounds our data suggest also that Ce(IV) coordinated by sulphate ligands may more easily be reduced than when it is surrounded by nitrato ligands. In fact, Ying and Rudong found that $Ce(SO_4)_2·4H_2O$ is reduced to $Ce_2(SO_4)_3$ when heated in air above 450°C [15].

In the case of the cerium ammonium sulphate the temperature needed for reduction is significantly lower, however.

One should note that the reaction equations (6–8 and 10–11) should be regarded as limiting cases expressing a unit change in the oxidation state of cerium. Taking into account the previous results suggesting a mixed oxidation state [17–22], the system may also be described by mixtures of compounds containing formally trivalent and tetravalent cerium.

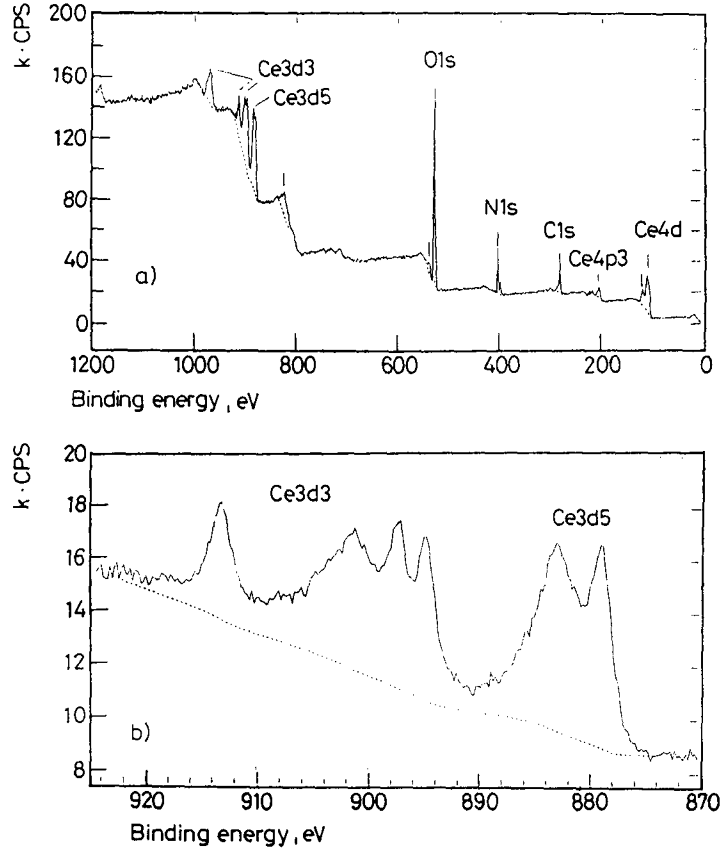

Fig. 6 Survey XPS spectra of a sample obtained by heating $(NH_4)_2Ce(NO_3)_6$ for 2 h at 210°C (above) and the Ce 3*d* transitions of the same spectra (below)

XPS study

A complete analysis of cerium 3*d* photoemission spectrum is complicated involving in partially reduced samples the analysis of ten peaks [37]. However, the well-defined $3d_{3/2}$ peak is due to Ce(IV) only and can be qualitatively used as a probe for the presence of Ce(IV) and the degree of reduction. Furthermore, XPS offers a more sensitive tool for the detection and possible determination of Ce(III) and Ce(IV) than magnetic susceptibility measurements.

In general, the results obtained were in agreement with the susceptibility measurements but, for example, the XPS data (Fig. 6) revealed, by the presence of the Ce $3d_{3/2}$ peak at 915 eV, that the sample assumed to be $Ce(NO_3)_3$ had partially decomposed to CeO_2.

Conclusions

The structure of (**1**) was solved from single crystal X-ray diffraction data and it appears to be isostructural with $K_4Ce(SO_4)_4 \cdot 2H_2O$. On heating (**1**) first looses the two molecules of water. The other intermediates and final products of the thermal decomposition of (**1**) and (**2**) are the same: $NH_4Ce(SO_4)_2$, $Ce(SO_4)_{3/2}$ and CeO_2. The intermediates and their temperature ranges do not depend on the inert or oxidative nature of the surrounding atmosphere. The latter, however, influences the heat effect of decomposition steps owing to the oxidation of ammonia. The occurrence of Ce(III) was proven by XPS and magnetic susceptibility measurements.

$Ce(NO_3)_3$ is probably an intermediate in the thermal decomposition of (**3**); large overlap between successive steps of the decomposition makes the isolation of the intermediate impossible, however. The presence of cerium(III) during the decomposition was proven by magnetic moment determination. The decomposition sequence of (**4**) includes $Cs_2CeO(NO_3)_4$, $Cs_2CeO_2(NO_3)_2$, Cs_2CeO_3 and CeO_2. The presence of Ce(IV) in the intermediates was proven by XPS and magnetic susceptibility measurements.

The differences among the compounds studied with regard to changes in cerium oxidation state can be explained by the reducing effect of ammonium ions. A comparison of our results as well as those of other authors [15] suggest that the sulfato ligand relative to nitrate also plays a role in the reduction process. This interesting finding of the Ce(IV) reduction in the presence of various ligands warrants a further study.

* * *

The authors wish to thank Dr. M. Näsäkkälä for magnetic moment determinations, Prof. V. Penttala for the TG–IR runs and Mr. M. Utriainen for the synthesis of 3. Dr. E. Ristolainen is thanked for recording the XPS spectra. During this study, G. P. received a scholarship from the Finnish Centre for International Mobility (Helsinki, Finland) under the agreement on scientific and cultural cooperation between Finland and Hungary; this scholarship is gratefully acknowledged.

References

1 B. Eriksson, L. O. Larsson, L. Niinistö and U. Skoglund, Inorg. Chem., 13 (1974) 290.

2 B. Eriksson, L. O. Larsson and L. Niinistö, Acta Chem. Scand., Ser. A, 36 (1982) 465.

3 M. Leskelä and L. Niinistö, in Handbook on the Physics and Chemistry of Rare Earths, Vol 8, eds. K. A. Gschneider and L. Eyring, North Holland, Amsterdam 1986, pp. 203–334.

4 L. Niinistö and M. Leskelä, *ibid.*, Vol. 9, 1987, pp. 91–320.

5 L. M. Dikareva, D. L. Rogachev, V. Ya. Kuznetsov and M. A. Porai-Koshits, Zh. Strukt. Khim., 26 (1985) 177; J. Struct. Chem. (Engl. transl.), 26 (1985) 303.

6 Gmelin Handbuch der Anorganischen Chemie, System-Nr. 39, Vol. C8, Springer Verlag, Berlin 1981, pp. 277–279.

7 D. L. Rogachev, R. K. Rastsvetaeva, V. Ya. Kuznetsov and L. M. Dikareva, Zh. Strukt. Khim., 30 (1989) 105; J. Struct. Chem. (Engl. transl.), 30 (1989) 620.

8 V. A. Golovnya and L. A. Pospelova, Zh. Neorg. Khim., 6 (1961) 636; Russian J. Inorg. Chem. (Engl. transl.), 6 (1961) 324.

9 S. E. Kharzeeva, A. S. Vyatkina and V. V. Serebrennikov, Zh. Neorg. Khim., 13 (1968) 1861; Russian J. Inorg. Chem. (Engl. transl.), 13 (1968) 969.

10 Atlas of Thermoanalytical Curves, Vol. 5, ed. Gy. Liptay, Akadémiai Kiadó, Budapest, Heyden and Son, London 1976, No. 306.

11 S. A. Bondar', N. L. Mikhailova, R. A. Popova and S. D. Nikitina, Zh. Neorg. Khim., 31 (1986) 625; Russian J. Inorg. Chem. (Engl. transl.), 31 (1986) 356.

12 S. A. Bondar', G. V. Trofimov, R. A. Popova and L. S. Korobeinikov, Izv. Akad. Nauk SSSR, Neorg. Mater., 18 (1982) 1209; Inorg. Mater. (Engl. transl.), 18 (1982) 1019.

13 J. E. House, Jr. and K. A. Kemper, Thermochim. Acta, 126 (1988) 407.

14 I. B. Sharma, V. Singh and M. Lakhanpal, J. Thermal Anal., 38 (1992) 1345.

15 Yang Ying and Yang Rudong, Thermochim. Acta, 202 (1992) 301.

16 V. Krasnikov, M. Vaivada and Z. Konstans, J. Solid State Chem., 74 (1988) 1.

17 F. Le Normand, L. Hilaire, K. Kili, G. Krill and G. Maire, J. Phys. Chem., 92 (1988) 2561.

18 L. Zhao, Wuli Huaxue Xuebao, 4 (1988) 71; Ref. Chem. Abstr. 108, 228874x, 1988.

19 L. Zhao, Wuli Xuebao, 38 (1989) 987; Ref. Chem. Abstr. 111, 243278m, 1989.

20 E. Abi-aad, R. Bechara, J. Grimblot and A. Aboukais, Chem. Mater., 5 (1993) 793.

21 A. Marcelli and A. Bianconi, Physica B, 158 (1989) 529.

22 N. Kuwano, Sogo Rikogaku Kenkyuka Hokuku (Kiushu Daigaku Daigakuin), 11 (1989) 195; Ref. Chem. Abstr. 112, 186144j, 1990.

23 P. N. Iyer and P. R. Natarajan, Thermochim. Acta, 210 (1992) 185.

24 T. A. Beineke and J. Delgaudio, Inorg. Chem., 7 (1968) 715.

25 F. Brezina and J. Rosicky, Monatsh. Chem., 94 (1963) 306.

26 M. I. Zaki and T. Baird, React. Solids, 2 (1986) 107.

27 W. W. Wendlandt, Anal. Chim. Acta, 15 (1956) 435.

28 S. Pajakoff, Monatsh. Chem., 95 (1964) 1108.

29 B. Claudel, Y. Trambouze and J. Veron, Bull. Soc. Chim. Fr., (1963) 409.

30 A. K. Molodkin, Z. K. Odinets, O. Vargas Ponse and B. E. Zaitsev, Russian J. Inorg. Chem. (Engl. transl.), 21 (1976) 1285.

31 C. A. Strydom and C. P. J. van Vuuren, J. Thermal Anal., 32 (1987) 157.

32 B. N. Ivanov-Emin and Yu. N. Medvedev, Russian J. Inorg. Chem. (Engl. transl.), 35 (1990) 168.

33 M. Karppinen, P. Kyläkoski, L. Niinistö and C. Rodellas, J. Thermal Anal., 35 (1989) 347.

34 T. Leskelä, M. Lippmaa, L. Niinistö and P. Soininen, Thermochim. Acta, 214 (1993) 9.

35 L. Hiltunen, G. Pokol, T. Leskelä and L. Niinistö, to be published.
36 L. Erdey, S. Gál and Gy. Liptay, Talanta, 11 (1964) 913.
37 M. Romeo, K. Bak, J. El Fallah, F. le Normand and L. Hilaire, Surf. Interface Anal., 20 (1993) 508.

Zusammenfassung — Zur Ermittlung des Zersetzungsmechanismus und zum Vergleich der Resultate mit den im Überblick angegebenen Literaturangaben wurden mittels simultaner TG/DTA unter verschiedenen Versuchsbedingungen vier Sulfato- und Nitratokomplexe von Zer(IV), nämlich von $(NH_4)_4Ce(SO_4)_4 \cdot 2H_2O$ (**1**), $(NH_4)_2Ce(SO_4)_3$ (**2**), $(NH_4)_2Ce(NO_3)_6$ (**3**) und $Cs_2Ce(NO_3)_6$ (**4**) untersucht. Im Falle der Ammoniumverbindungen (**1**, **2** und **3**) werden die Zersetzungen von Änderungen des Oxidationszustandes von Zer begleitet; die Gegenwart von Ce(III) und Ce(IV) wurde durch ex situ Messungen der magnetischen Suszeptibilität und durch XPS-Messungen untersucht. Weiterhin wurde auch die Kristallstruktur von **1** ermittelt. Diese Verbindung bildet monoklinische Kristalle der Raumgruppe $P2_1/c$; die Parameter der Elementarzelle lauten: a = 12.638(18) Å, b = 11.362(10) Å, c = 13.607(11) Å, ß = 110.17(9), V = 1834.05 $Å^3$.